

Fig. 1 Comparison of square-root estimates with covariance (Kalman-Bucy) estimates.

motion assumed for the comparison are a realistic approximation to the equations which govern the shuttle vehicle during the post-blackout maneuver. A complete description of the equations of motion and the observation-state relations used in the simulation described here is given in Ref. 8. In this investigation, the triangular state-error covariance algorithm discussed in the previous section was combined with a Carlson square-root measurement update algorithm⁵ to obtain a complete filter algorithm. This algorithm was implemented in the computer simulation program described in Ref. 8. Figure 1 shows the variation with time of the position error norm $\Delta r = (\Delta x^2 + \Delta y^2 + \Delta z^2)^{1/2}$ and the associated state-error covariance matrix norm $(P_{xx} + P_{yy} + P_{zz})^{1/2}$ as determined by the conventional Kalman-Bucy filter. In Fig. 1b, the error norm and the covariance matrix norm obtained with the square-root filter are shown. The covariance matrix P for the square-root filter was obtained using the relation $\bar{P} = WW^T$, i.e., Eq. (3). Note that the norm of the covariance matrix position elements is essentially identical for both methods. There are slight differences in the position error norm estimates prior to the 3 min epoch. After this time period, the position error estimates for both algorithms are essentially the same. Similar results were obtained for the estimates of the velocity components. Finally the investigation indicates that, using the UNIVAC 1107 at the NASA Johnson Spacecraft Center, the square-root filter algorithm obtained by combining the triangular covariance matrix propagation algorithm with the triangular measurement update algorithm described in Ref. 5 requires a computation time which exceeds that required by the standard Kalman-Bucy filter by less than 15%.

References

- 1 Kalman, R. E. and Bucy, R. S., "New Results in Linear Filtering and Prediction," *ASME Transactions, Journal of Basic Engineering*, Ser. D, Vol. 82, 1960, pp. 35-45.

² Battin, R. H., *Astronautical Guidance*, McGraw-Hill, New York, 1964, pp. 388-389.

³ Bellantoni, J. F. and Dodge, K. W., "A Square Root Formulation of the Kalman-Schmidt Filter," *AIAA Journal*, Vol. 5, July 1967, pp. 1309-1314.

⁴ Kaminski, P. G., Bryson, A. E., and Schmidt, S., "Discrete Square Root Filtering, A Survey of Current Techniques," *IEEE Transactions on Automatic Control*, Vol. AC-16, 1971, pp. 727-736.

⁵ Carlson, N. A., "Fast Triangular Formulation of the Square Root Filter," *AIAA Journal*, Vol. 11, Sept. 1973, pp. 1239-1265.

⁶ Andrews, A., "A Square-Root Formulation of the Kalman Covariance Equations," *AIAA Journal*, Vol. 6, June 1968, pp. 1165-1166.

⁷ Tapley, B. D., Choe, C. Y., and McMillan, J. D., "A Triangular Square-Root Sequential Estimation Algorithm," *Proceedings of the Fifth Symposium on Nonlinear Estimation and Its Applications*, IEEE Control Systems Society, San Diego, Calif., Sept. 23-25, 1974.

⁸ Lear, W. M., "A Prototype Real-Time Navigation Program for Multi-Phase Missions," TRW Rept. 17618-6003-T0-00, Dec. 1971, TRW Systems Group, Redondo Beach, Calif.

Velocity and Shear-Stress in a Transpired Turbulent Boundary Layer

C. G. KOOP*

University of Southern California, Los Angeles, Calif.

Introduction

IN recent years there has been considerable effort devoted to the study of turbulent boundary-layer flows over porous surfaces with mass transfer. There have been methods developed for calculating such flows, but these studies have had to rely upon extensive numerical schemes, or only yielded information about the gross features of the boundary layer such as momentum or displacement thickness. The present method presents a simple means of predicting not only the gross parameters, but also distributions of velocity and Reynolds stress through the turbulent boundary layer.

Theory and Results

For a two-dimensional turbulent boundary-layer flow with zero pressure gradient, the governing equations of continuity and momentum are given by

$$(\partial u / \partial x) + (\partial v / \partial y) = 0 \quad (1)$$

$$u(\partial u / \partial x) + v(\partial u / \partial y) = (1/\rho)(\partial \tau / \partial y) \quad (2)$$

where ρ is the fluid density, and τ is the sum of the laminar shear stress τ_l and the turbulent shear stress τ_t .

The boundary conditions to be imposed upon Eqs. (1) and (2) are given by

$$u(x, 0) = 0, \quad u(x, \delta) = U_\infty, \quad v(x, 0) = V_w \quad (3)$$

where δ and U_∞ are the boundary-layer thickness and freestream velocity, respectively. V_w is the transpiration velocity at the wall. It is assumed that a similarity solution to Eqs. (1) and (2) exists, and has the form

$$u(x, y) = U_\infty f(\eta) \\ \eta(x, y) = y/\delta(x) \quad (4)$$

Using Eq. (4) and the momentum integral equation, streamwise derivatives may be written as

$$\partial / \partial x = -(C_f/2\theta)(1+B)\eta(d/d\eta) \quad (5)$$

Received June 7, 1974; revision received September 27, 1974. The help and advice of Dr. T. Cebeci is gratefully acknowledged.

Index category: Boundary Layers and Convective Heat Transfer—Turbulent.

* Graduate Research Assistant, Department of Aerospace Engineering.

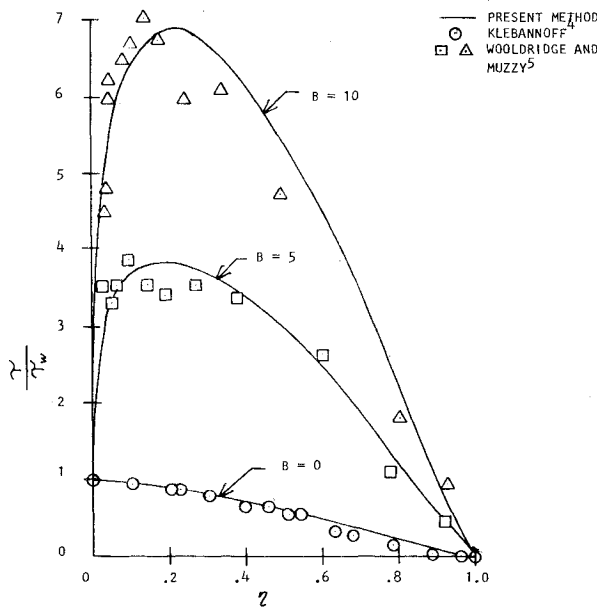


Fig. 1 Comparison of theoretical and experimental profiles of shear stress.

where C_f is the local skin friction, θ is the momentum thickness, and B is given by:

$$B = 2\bar{V}_w/C_f, \quad \bar{V}_w = V_w/U_\infty$$

Substituting Eqs. (4) and (5) into Eqs. (1) and (2) and combining yields

$$\frac{\tau}{\tau_w} = \left\{ (1+Bf) - \frac{R_\delta}{R_\theta} (1+B) \left[f \int_0^\eta f(\xi) d\xi - \int_0^\eta f^2(\xi) d\xi \right] \right\} \quad (6)$$

where τ_w is the wall shear stress, and R_δ and R_θ are the Reynolds numbers based upon boundary-layer thickness and momentum thickness, respectively.

Using Prandtl's mixing-length theory with the sublayer correction suggested by Van Driest¹ and a further modification presented by Cebeci² to account for the mass transfer at the wall, the shear stress τ is given by

$$\tau = \rho v \frac{\partial u}{\partial y} + \rho (ky)^2 [1 - \exp(-y/A)]^2 \left(\frac{du}{dy} \right)^2 \quad (7a)$$

where

$$A = A^+ v (\tau_w/\rho)^{-1/2} \exp(-5.9B) \quad (7b)$$

and v is the kinematic viscosity. k and A^+ are empirical constants equal to 0.40 and 26, respectively, for $R_\theta > 2000$. For $R_\theta < 2000$, their functional dependence upon Reynolds number is given by Koop.³

Using Eqs. (7a) and (7b) for the shear stress with a correction in the wake region of the boundary layer suggested by Coles,⁴ and substituting into Eq. (6), yields

$$\begin{aligned} df/d\eta = & \left\{ -1/R_\delta + [(1/R_\delta)^2 - 4ac]^{1/2}/2a \right\} - \\ & (C_f G/k) 2\pi \sin[(\pi/2)\eta] \cos[(\pi/2)\eta] \\ a = & (k\eta)^2 \left\{ 1 - \exp \left[-\frac{\eta R_\delta (C_f/2)^{1/2}}{A^+} \exp(-5.9B) \right] \right\} \end{aligned} \quad (8)$$

$$C = \frac{-C_f}{2} \left[1 + Bf - \frac{R_\delta}{R_\theta} (1+B) \left(f \int_0^\eta f(\xi) d\xi - \int_0^\eta f^2(\xi) d\xi \right) \right]$$

subject to boundary conditions given by:

$$f(0) = 0; \quad \left. \frac{df}{d\eta} \right|_{\eta=0} = R_\delta C_f/2; \quad f(1) = 1 \quad (9)$$

For $R_\theta > 4000$, $G = 0.55$. For $R_\theta < 4000$ its functional dependence upon R_θ is given by Koop.³

It can be seen that Eqs. (8) and (9) contain the 4 parameters \bar{V}_w , C_f , R_δ and R_θ . However, R_δ and R_θ are related by

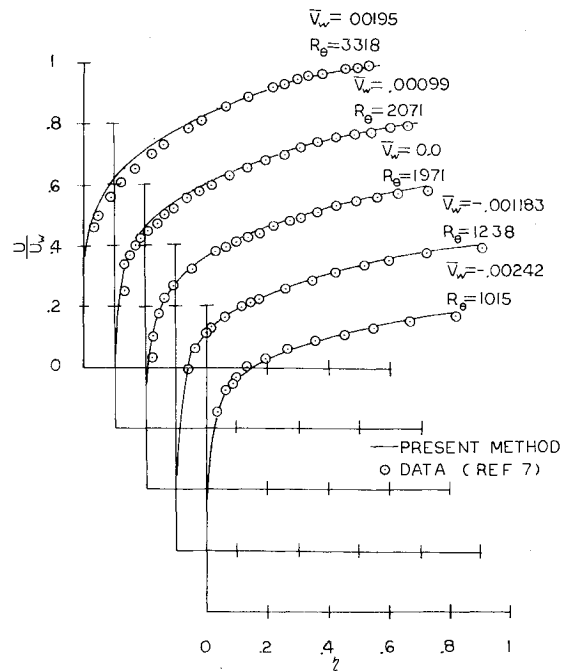


Fig. 2 Velocity profiles for zero mass transfer and moderate mass transfer rates—low Reynolds number.

$$R_\theta = R_\delta \int_0^1 f(\eta)[1 - f(\eta)] d\eta \quad (10)$$

Thus, given any 2 parameters, say \bar{V}_w and R_θ , Eqs. (8–10) constitute a nonlinear eigenvalue problem with eigenvalues C_f and R_δ and eigenvector $f(\eta)$. Using Newton's variational method and a Runge-Kutta integration scheme, Eqs. (8–10) were solved numerically. The calculated results for the velocity and shear-stress distribution are presented in Figs. 1–3, along with the experimentally measured values of Wooldridge and Muzzy,⁵ Klebanoff,⁶ and Simpson.⁷ The calculated eigenvalues C_f and R_δ are presented in Table 1 and are compared with the measurements of Simpson.⁷

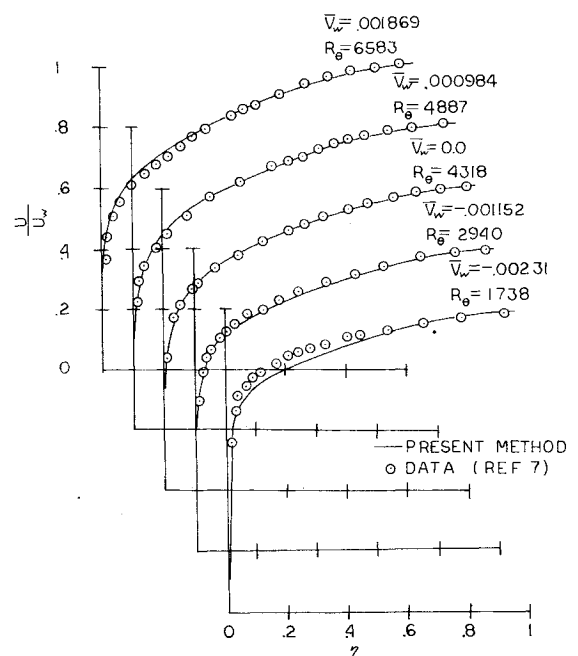


Fig. 3 Velocity profiles for zero mass transfer and moderate mass transfer rates—high Reynolds number.

Table 1 Comparison of calculated and experimental values of C_f and R_δ

\bar{V}_w	$R_\delta \times 10^{-3}$	C_f		$R_\delta \times 10^{-4}$	
		Experimental (Ref. 7)	Calculated	Experimental (Ref. 7)	Calculated
0	1.971	0.00392	0.00397	1.88	1.89
	4.318	0.00326	0.00317	3.88	3.97
-0.00118	1.238	0.00520	0.00539	1.28	1.31
	2.94	0.00440	0.00437	3.06	2.90
-0.00242	1.015	0.00622	0.00671	1.285	1.20
	1.738	0.00566	0.00596	2.27	1.90
-0.00465	0.191	0.00920	0.00922	0.39	0.22
0.00099	2.071	0.00336	0.00332	1.71	1.91
	4.887	0.00272	0.00255	4.02	4.30
0.00195	3.318	0.00244	0.00242	2.56	2.84
	6.583	0.00202	0.00201	5.05	5.58
0.00388	4.518	0.00148	0.00163	3.10	3.59
	9.429	0.00114	0.00147	6.62	7.37
0.00780	9.732	0.00036	0.00094	5.87	6.97
	15.935	0.00024	0.00082	10.00	11.50

References

- Van Driest, E. R., "On Turbulence Flow Near a Wall," *Journal of the Aeronautical Sciences*, Vol. 23, Nov. 1956, pp. 1007-1011.
- Cebeci, T., "The Behavior of Turbulent Flow Near a Porous Wall with Pressure Gradient," DAC-70014, May 1970, Douglas Aircraft Co., Long Beach, Calif.
- Koop, C. G., "Calculation of the Velocity and Shear-stress Profiles for Flat-Plate Incompressible Turbulent Boundary-Layer Flows With and Without Mass Transfer," M.S. thesis, 1971, Mechanical Engineering Dept., California State University, Long Beach, Calif.
- Coles, D., "The Law of the Wake in the Turbulent Boundary-Layer," *Journal of Fluid Mechanics*, Vol. 1, Pt. 1, June 1956, pp. 191-226.
- Wooldridge, C. E. and Muzzy, R. J., "Boundary-Layer Turbulence With Mass Addition and Combustion," *AIAA Journal*, Vol. 4, Nov. 1966, pp. 2009-2016.
- Klebanoff, D. S., "Characteristics of Turbulence in a Boundary Layer with Zero Pressure Gradient," TN 3178, July 1954, NACA.
- Simpson, R. L., "The Turbulent Boundary Layer on a Porous Plate: An Experimental Study of the Fluid Mechanics With Injection and Suction," Ph.D. thesis, 1967, Dept. of Mechanical Engineering, Stanford University, Palo Alto, Calif.

Effects of Constraint Modification on the Random Vibration of Damped Linear Structures

L. J. HOWELL*

General Motors Corporation, Warren, Mich.

Introduction

MOTIVATED by a desire for enhanced computing efficiency, numerous investigators have recently explored techniques for assessing the effects of system modification on structural vibration. Such techniques could also provide a foundation upon which efficient optimization algorithms might be

Received July 3, 1974; revision received November 11, 1974. The author wishes to express his appreciation to the reviewers for the comments and helpful suggestions which were used in preparing this Note.

Index category: Structural Dynamic Analysis.

*Supervisory Research Engineer, Engineering Mechanics Department. Member AIAA.

developed. Much of the reported research has dealt with procedures necessary to determine the eigenvalues and eigenvectors of the modified system by utilizing available information concerning the original system. For example, such methods which are applicable for treating damped linear systems are discussed in Ref. 1.

Dowell² has described a procedure for computing the vibration modes of a structure whose support conditions are modified. The method uses the normal modes of the original system in a Rayleigh-Ritz analysis with the new constraints enforced by Lagrange multipliers. His technique has obvious potential for treating the synthesis of large structures whose components are defined in terms of their unconstrained modes.³ Hallquist and Snyder⁴ have recently extended Dowell's work to include viscous damping.

In the present Note, we have utilized the results of Refs. 2 and 4 to formulate a direct solution for the stationary random response of the modified system. Specifically, the matrix of cross-spectral density functions for the modified system is written in terms of the cross-spectral density matrix of the original system, the frequency response functions for the original system, and the parameters describing the added constraints. These new results are believed to have significant practical application, particularly since computer programs could be used to generate directly the transfer functions and cross-spectral density functions—these might then be stored and used in a post-processor scheme to determine the random vibration of the modified system.

Analysis

Consider a dynamic system with n degrees of freedom. Let the characteristics of the linear system be defined by the generalized mass, stiffness, and damping matrices $[M]$, $[K]$, and $[C]$. Assume that the structure is to be constrained by g rigid supports and h elastic supports. The displacements of the nonrigid supports at the support-structure attachment points will be designated $\{p\}$. The support modifications can be described by the k constraint relations:

$$\{f\} = [\beta] \{q\} - \begin{Bmatrix} \{0\} \\ \{p\} \end{Bmatrix} = \{0\} \quad (1)$$

where $[\beta]$ defines the type of modification and $\{q\}$ is the vector of generalized coordinates for the unconstrained (or less constrained) structure. Note that $k = g + h$. A Lagrangian formulation yields n equations of the form^{2,4}

$$[M] \{\ddot{q}\} + [C] \{\dot{q}\} + [K] \{q\} - [\beta]^T \{\lambda\} = \{Q\} \quad (2)$$

and h equations

$$[\bar{K}_s] \{p\} = -\{\lambda_1\} \quad (3)$$

where Q_i are the generalized forces and $[\bar{K}_s]$ defines the stiffnesses of the h elastic constraints. (For simplicity we have assumed that the elastic constraints are individually grounded.) The total set of Lagrange multipliers, $\{\lambda\}$, consists of those which define rigid constraint forces $\{\lambda_0\}$ and those which define elastic constraint forces $\{\lambda_1\}$. Thus,

$$\{\lambda\} = \begin{Bmatrix} \{\lambda_0\} \\ \{\lambda_1\} \end{Bmatrix}$$

The applicable constraint relations, k in number, are

$$[\beta] \{q\} = \begin{Bmatrix} \{0\} \\ \{p\} \end{Bmatrix} \quad (4)$$

where $\{p\}$ may be written in terms of the Lagrange multipliers $\{\lambda_1\}$ by using Eq. (3).

Usually, Eq. (2) will be coupled because of the presence of off-diagonal terms in the mass, stiffness, or damping matrices. However, the system can be uncoupled by introducing the transformation⁵

$$\{z\} = \begin{Bmatrix} \{\dot{q}\} \\ \{q\} \end{Bmatrix} = [\Phi] \{\xi\} \quad (5)$$

Equations (2) and (4) then become⁴

$$[\bar{I}] \{\ddot{\xi}\} - [\bar{\mu}] \{\dot{\xi}\} - [\bar{W}]^T \{\lambda\} = \{\bar{F}\} \quad (6)$$